

Equation of State and Phase Diagram of Solid ^4He from Single-Crystal X-ray Diffraction over a Large P - T Domain

P. Loubeyre, R. LeToullec, and J. P. Pinceaux

Physique des Milieux Condensés and Université Paris 6, boîte 77, 4 place Jussieu, 75252 Paris, France

H. K. Mao, J. Hu, and R. J. Hemley

Geophysical Laboratory and Center for High Pressure Research, Carnegie Institution of Washington, 5251 Broad Branch Road N.W., Washington, D.C. 20015

(Received 17 February 1993)

Single-crystal x-ray diffraction has been performed on solid ^4He from 1 to 58 GPa over the temperature range 46–400 K. The high-density properties of helium are pinned down: the hcp structure is stable apart from an fcc loop along melting in between 15 K and around 285 K; comparison of the 304 K hcp equation of state with a series of calculations demonstrates there are significant attractive many-body interactions; and the thermal pressure has been measured between 95 and 304 K and it differs from self-consistent phonon calculations.

PACS numbers: 67.80.Gb, 61.10.Lx, 62.50.+p

The determination of the structural properties of He has been a topic of continuous interest because of its quantum nature, electronic simplicity, and astrophysical relevance. At low pressure, solid He has been extensively studied as a model system for strongly anharmonic solids [1]. A related property is the existence of the fcc-hcp phase transition that has been measured up to 1 GPa [2]. With the decrease of anharmonicity under pressure, the hcp phase line [3,4] was predicted to curve back on the pressure axis, fcc becoming the stable structure as in the heavier rare gas solids. Recent advances in diamond-anvil cell technology have enabled measurements of properties of He at very high pressure. The measurement of the melting curve [5] suggested the possibility of other phase transitions at high pressure. This behavior was also examined in subsequent theoretical calculations [6–8]. Definitive answers to these questions can be obtained by direct crystal structure determination, such as that provided by x-ray diffraction. Mao *et al.* overcame the problem arising from both the extremely low scattering cross section of helium atoms and the small volume of diamond-cell samples at very high pressures [9]: They found the hcp structure to be stable from 15 to 23 GPa at ambient temperature, in contrast to theoretical predictions. The present study was undertaken to complete the determination of the phase diagram of ^4He over a large P - T domain and to examine the unusual behavior of He in its very high-density states.

The method of measuring x-ray diffraction of ultralight elements, such as He and H_2 , under high pressure in a diamond cell involves a combination of single-crystal and energy-dispersive diffraction techniques with synchrotron polychromatic radiation. The room temperature technique is described elsewhere [9,10]. Briefly, the cell is centered on a χ rotation stage that is fixed on a goniometer head to provide ω rotation. The Ge solid state detector measures reflections at a fixed 2θ angle (in the present measurements set to 20°). A peak is found in the

energy-dispersive x-ray spectrum when the diffraction conditions are satisfied for a specific combination of χ and ω . A novel system was designed to extend such measurements to variable temperature. As described in detail previously [11], it consists of a membrane diamond cell for x ray and a helium flow cryostat with an *in situ* rotator. Two design characteristics are crucial for the variable temperature technique. First, the x-ray viewing angle of both sides of the sample is kept as large as $\pm 45^\circ$. Second, during the ω rotation of the cryostat and the χ rotation of the cell inside the cryostat, the eccentricity was required to be less than $30\ \mu\text{m}$. The peaks could thus be searched by an automatic step scanning of the rotation angles χ and ω , the small eccentricity enabling the collimated x-ray beam (from 20 to $50\ \mu\text{m}$ square) always to impinge on the sample. When a He diffraction peak was found during a typical operation, optimization of the diffraction angles resulted in typically very high signal to noise ratio. Single-crystal diffraction of helium could be distinguished from that of ruby and the diamond anvils and from the polycrystalline diffraction of the stainless-steel gasket by spatial resolution. The membrane diamond cell was loaded in a high pressure vessel at room temperature with high purity He gas ($\geq 99.99\%$). A small ruby sphere ($10\ \mu\text{m}$ in diameter) was put at the edge of the sample chamber. Measurements were performed on the X17C superconducting wiggler beam line at the National Synchrotron Light Source (Brookhaven National Laboratory) during four runs over a period of two years. The uncertainty in the volume measurement, estimated to be less than 0.4%, originates principally from the uncertainty in the calibration of the 2θ angle, and to a lesser degree from the energy calibration of the Ge detector and from centering of the reflections. Pressures were measured in the hutch by ruby fluorescence excited with a Cd laser using the quasihydrostatic ruby scale [12] including variable temperature corrections [13]. Fine adjustments and accurate measurements of

pressure ($\Delta P = \pm 0.1$ GPa) and temperature ($\Delta T = \pm 0.5$ K) could be performed inside the hutch without misaligning the sample.

The structural properties of ^4He were explored over the temperature range of 46–400 K and as a function of pressure up to 58 GPa. Single crystals filling the whole sample chamber could be grown from the melt by isochoric scans. Their dimensions were typically 200 μm in diameter and 40 μm in thickness for pressures below 15 GPa (using 550 μm culets) and 100 μm in diameter and 15 μm in thickness for reaching 60 GPa (using bevel diamonds with 200 μm central flat). Single crystals were stabilized a few degrees below melting for x-ray characterization. The resulting x-ray reflections were very sharp (rocking angle in ω typically about 0.03°), indicative of high quality crystals. The reflections were indexed from their angular position and the d spacings. The χ and ω positions of the reflections reachable within the angular aperture of the cell were calculated from the orientation matrix. The volume was determined from selected d spacings.

Figure 1 shows the P - T range of crystals identified as fcc and hcp. The fcc-hcp transition line was explored by varying the P - T conditions. Starting from single crystals of the fcc phase, the pressure was increased at constant temperature at 64 and 247 K and the temperature changed at constant pressure at 8 GPa. In each case, a gradual decrease in the intensity of the followed fcc reflections, belonging to the 111 and 200 classes, was observed until they disappeared. Starting with the two hcp

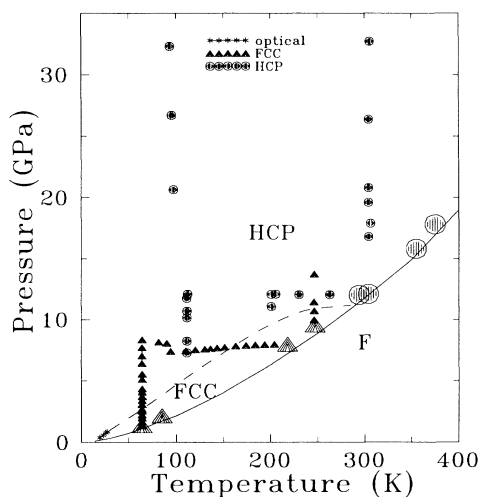


FIG. 1. Phase diagram of ^4He . The large dots and large triangles, respectively, correspond to single crystals of the hcp and fcc structures, for which the orientation matrix was found. The small symbols indicate the P - T points where the diffraction peaks of these single crystals under varied thermodynamic conditions could be measured. The dashed line is the hcp-fcc phase line. The stars indicate the large volume optical measurements of this transition [2]. The full line is the Simon melting equation [15].

single crystals characterized around 300 K, the temperature was first decreased to 200 K in one case and 100 K in the other. The pressure was then decreased at constant temperature; each time, the reflections were lost after a large decrease of pressure. It should be noted that after the total disappearance of the diffraction peaks of the parent single crystal (either hcp or fcc), no peak of the product crystal could be found. We suggest that the single crystals are broken at the fcc-hcp phase transition. This contrasts with the behavior observed optically at low pressures in large volume studies [14]. Starting from single crystals of the hcp phase at 355 and 375 K, the temperature was stabilized at 304 or 95 K and the pressure was increased to 58 GPa; no significant weakening of the hcp peaks was observed although the peaks broaden up to a $\Delta\omega$ of 0.4° . Solid He remained a single crystal up to the maximum pressure.

In Fig. 1, the small triangles and the small dots indicate the P - T points where diffraction peaks of the fcc and the hcp structures were measured. There exists a P - T region over which either fcc or hcp structures can be stabilized, depending on the thermodynamic path used to reach this state. We propose that strong hysteresis arises from the martensitic mechanism of the fcc-hcp transformation, which involves motion of planes of atoms (e.g., very likely through Shockley partial dislocation [2,14]). Because of the hysteresis, precise determination of the equilibrium transition line is difficult (especially in view of the limitation on synchrotron beam time). Our best estimate of the phase line is drawn in Fig. 1, which is fully consistent with the optical determination of Franck and Daniels [2]. The present study demonstrates that the fcc domain is limited in a loop along melting in between 15 and 285 K (± 15 K). Such a topology is very unusual. The anomaly [5] reported on the melting curve of ^4He , although not seen in a subsequent investigation [15], should thus correspond to the fcc-hcp-fluid triple point, instead of the fcc-bcc-fluid one as suggested by earlier calculations [6–8]. The hcp structure is stable along the melting curve up to the highest temperature reached here (400 K). This does not rule out the possible existence of the bcc phase along melting at higher temperatures but it places a lower bound on a possible hcp-bcc-fluid triple point. Finally, the hcp structure is seen to be stable up to 58 GPa. This experimental phase diagram for ^4He differs from theoretical predictions. The growing importance of many-body interactions may be responsible for stabilizing the hcp structure at high pressure [8]. The hcp structure is stable in xenon at high pressure [16]. However, it is intriguing that such a hcp structure is not observed in Ne [17], Ar [18], and Kr [19] solids at high pressure since their many-body interactions, associated with the deformation of the atomic electronic cloud, should be even more important and of roughly the same form in comparison to He.

The pressure variation of the lattice parameters of the hcp structure at 304 K was measured in two different

runs. For each pressure, the volume was estimated from at least three diffraction peaks [in one case indexed as (010), (011), and (002) and in the other case as ($1\bar{1}0$), ($1\bar{1}1$), ($1\bar{1}2$), and ($2\bar{1}0$)]. No systematic change with pressure of the c/a ratio is detected, with values scattered within ± 0.005 around 1.630, close to the ideal value. The measured volumes are compared in Fig. 2 with the previous measurements of Mao *et al.* [9] and with four calculated equations of state (EOS). The pressures calculated using self-consistent phonon calculation [8] with the HFD-B Aziz pair potential [20] are increasingly higher with density than experimental data because the growing importance of many-body interactions introduces a softening in the equation of state. These many-body interactions are implicitly included in the Ross-Young pair potential [21] (fitted on shock experiments) which leads to a better agreement with experiment, although it is increasingly discrepant above 20 GPa. Two models have been proposed to take explicitly into account these many-body interactions. In the first one [22], the softening of the pair potential is attributed to the contraction of the electronic cloud of He atoms in the crystal field calculated by a Gordon-Kim Hartree-Fock method. In the second [8], the deviation from the pair interaction is attributed to the three-body interaction and its effect calculated by perturbation over the pair potential phonon calculation. These two theoretical calculations bound the experimental data, neither being entirely satisfactory. The pressure increasing difference between experiment and the three-body calculation could suggest the need for higher order terms in the multibody expansion of interaction energy.

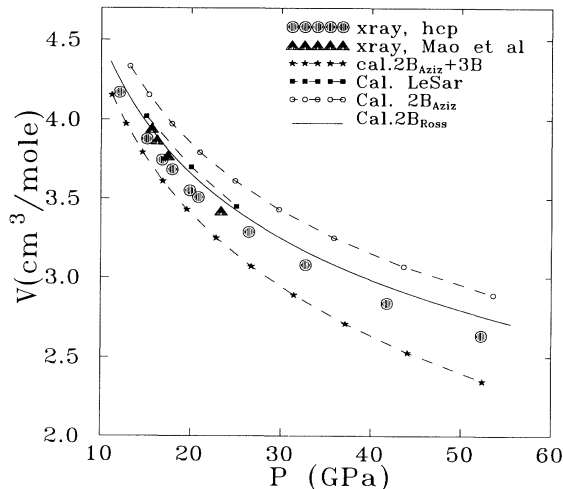


FIG. 2. Volume versus pressure data of hcp ^4He at 304 K. The dots indicate the present x-ray measurements and the triangles are from Mao *et al.* [9]. Four calculated equations of state are compared: self-consistent phonon calculations either with the HFD-B pair potential (dash-dotted line), the Ross-Young potential (full line), the HFD-B pair potential, plus three-body interaction (dashed-stars line). The dashed-squares line is a Gordon-Kim/Hartree-Fock calculation of LeSar [20].

Driessen, van der Poll, and Silvera [23] have determined a very accurate EOS of ^4He for volumes larger than $6 \text{ cm}^3/\text{mole}$, based on the data in the literature and their isochoric measurements. They tentatively extended it to $2.5 \text{ cm}^3/\text{mole}$. The Mie-Gruneisen model was used to fit the thermal pressure. This form for the thermal pressure is in very good agreement up to $2.5 \text{ cm}^3/\text{mole}$ with our self-consistent phonon calculations using the Ross-Young potential. Accordingly in Fig. 3 we have reduced all our pressure-volume data to $T=0 \text{ K}$, either in the fcc or the hcp phase. The EOS of Driessen, van der Poll, and Silvera (valid above $10 \text{ cm}^3/\text{mole}$) is in very good agreement with the data above $6 \text{ cm}^3/\text{mole}$ but the agreement is less satisfactory at smaller volumes. This illustrates that a third order Birch-Murnaghan form is not suitable for a large domain of compression [24]. The dashed line represents the Vinet function [25], which was fitted with the present data by a three parameters adjustment, giving $V_0(\text{cm}^3/\text{mole})=13.72$, $K_0(\text{GPa})=0.225$, and $K'_0(\text{GPa})=7.35$. It reproduces experiment to within 5% from 8 to $2.5 \text{ cm}^3/\text{mole}$. However, such a form does not represent the EOS of ^4He over a larger volume domain (the entire volume domain now investigated in ^4He is $21\text{--}2.5 \text{ cm}^3/\text{mole}$). It should be noted that below 20 GPa the dispersion of the data corresponds almost to the error bars and no volume difference between fcc and hcp structures is detected. As seen below, the dispersion of the reduced ($T=0 \text{ K}$) data above 20 GPa can be attributed to the nonphonon type thermal effects at high pressure.

The volume of hcp ^4He versus pressure measured at 95 and 304 K are compared in Fig. 4. A thermal difference is clearly measurable (it is much greater than the experi-

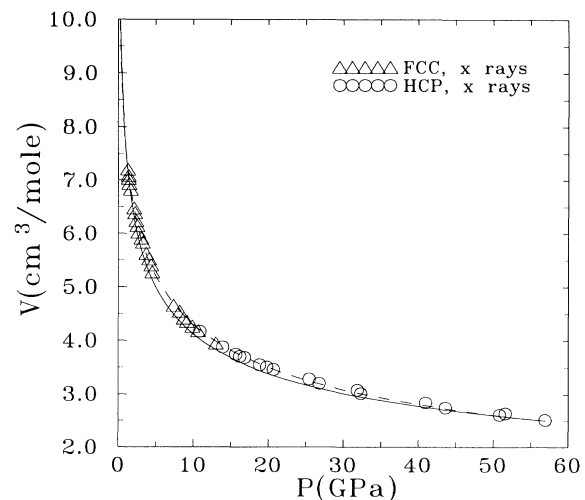


FIG. 3. Temperature reduced ($T=0 \text{ K}$) equation of state of solid ^4He . The dots and triangles represent the data for the hcp and fcc phases, respectively; the full line is the EOS of Driessen, van der Poll, and Silvera [23]. The dashed line is the Vinet form fit to the present data [$V_0(\text{cm}^3/\text{mole})=13.72$; $K_0(\text{GPa})=0.225$; $K'_0(\text{GPa})=7.35$].

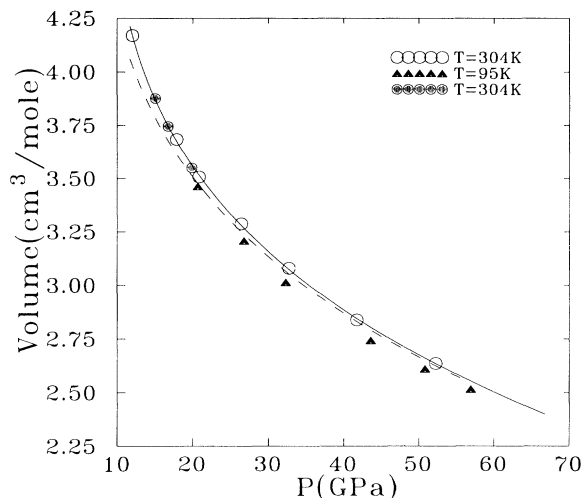


FIG. 4. Comparison between the $T=95$ K and the $T=304$ K volume versus pressure data of hcp ^4He . The $T=95$ K measurements are indicated as triangles and the $T=304$ K ones as circles; full and open symbols indicate two different experiments. The full line is a fit of the 304 K data. The dashed line is the expected EOS at 95 K obtained by adding the self-consistent phonon thermal corrections to the EOS at 304 K.

mental uncertainty which is of the order of the dispersion of the data obtained from different runs). Furthermore, the 95 K data were obtained on the same single crystal during the same run (i.e., with the same angle and energy calibrations) as one of the 304 K data set. Three peaks were followed [indexed as $(1\bar{1}0)$, $(1\bar{1}1)$, $(1\bar{1}2)$]. The 304 K data can be fit very well with a third order polynomial in density, as shown in the figure. The 95 K EOS is calculated by adding to the 304 K EOS the thermal pressures determined from the self-consistent phonon calculation with the Ross-Young potential. Around 20 GPa, the experimental thermal shift is in good agreement with the calculated one but above, experiment increasingly differs from calculation, being systematically larger. This discrepancy cannot be attributed to the model, since a self-consistent phonon calculation is expected to be accurate [26], nor to the use of the assumed pair potential. Similar results are obtained using the Aziz HFD-B potential or the pair potential adjusted on the 304 K EOS. We suggest that the presence of strong many-body interactions at high density gives rise to dynamical properties that are not adequately described using pairwise interactions (i.e., described at the self-consistent phonon level). This behavior may be also related to the presence of unusual quantum effects in dense helium inferred from the recent finding of an abnormal isotopic shift on the melting curve of He at high density [27]. This question should continue to motivate further investigations of the properties of dense low- Z solids. In this respect, the same x-ray study on solid ^3He should be very enlightening.

This work was supported by NATO Scientific Affairs Division under Grant No. CRG-890084, by the Commissariat à l'Énergie Atomique under Grant No. DAM/

CEL-2561/3272, NSF, and NASA. Technical support from NSLS is appreciated. We thank J. M. Besson and L. W. Finger for continued interest. Physique des Milieux Condensés is CNRS URA 782.

- [1] H. R. Glyde, in *Rare Gas Solids*, edited by M. L. Klein and J. A. Venables (Academic, New York, 1974), p. 382.
- [2] J. P. Franck and W. B. Daniels, *Phys. Rev. Lett.* **44**, 259 (1980); *Phys. Rev. B* **24**, 2456 (1981).
- [3] B. L. Holian, W. D. Gwinn, A. C. Luntz, and B. J. Alder, *J. Chem. Phys.* **59**, 5444 (1973).
- [4] P. Loubeyre, *Phys. Lett. A* **125**, 215 (1987).
- [5] P. Loubeyre, J. M. Besson, J. P. Pinceaux, and J. P. Hansen, *Phys. Rev. Lett.* **49**, 1172 (1982).
- [6] D. A. Young, A. K. McMahan, and M. Ross, *Phys. Rev. B* **24**, 5119 (1981).
- [7] D. Levesque, J. J. Weis, and M. L. Klein, *Phys. Rev. Lett.* **51**, 670 (1983).
- [8] P. Loubeyre, *Phys. Rev. Lett.* **58**, 1857 (1987).
- [9] H. K. Mao, R. J. Hemley, Y. Wu, A. P. Jephcoat, L. W. Finger, C. S. Zha, and W. A. Bassett, *Phys. Rev. Lett.* **60**, 2649 (1988).
- [10] H. K. Mao, A. P. Jephcoat, R. J. Hemley, L. W. Finger, C. S. Zha, R. M. Hazen, and D. E. Cox, *Science* **239**, 1131 (1988).
- [11] R. LeToullec, P. Loubeyre, J. P. Pinceaux, H. K. Mao, and J. Hu, *High Pressure Res.* **6**, 379 (1992).
- [12] K. H. Mao, J. Xu, and P. M. Bell, *J. Geophys. Res.* **91**, 4673 (1986).
- [13] D. E. McCumber and M. D. Sturge, *J. Appl. Phys.* **34**, 1682 (1963).
- [14] K. A. McGreer, K. R. Lundgreen, and J. P. Franck, *Phys. Rev. B* **42**, 87 (1990).
- [15] W. L. Vos, M. G. E. van Hinsberg, and J. A. Schouten, *Phys. Rev. B* **42**, 6106 (1990).
- [16] A. P. Jephcoat, H. K. Mao, L. W. Finger, D. E. Cox, R. J. Hemley, and C. S. Zha, *Phys. Rev. Lett.* **59**, 2670 (1987).
- [17] R. J. Hemley, C. S. Zha, A. P. Jephcoat, H. K. Mao, L. W. Finger, and D. E. Cox, *Phys. Rev. B* **39**, 11820 (1989).
- [18] M. Ross, H. K. Mao, P. M. Bell, and J. Xu, *J. Chem. Phys.* **85**, 1028 (1986).
- [19] A. Polian, J. M. Besson, M. Grimsditch, and W. A. Grosshans, *Phys. Rev. B* **39**, 1332 (1989).
- [20] R. A. Aziz, F. R. W. McCourt, and C. C. K. Wong, *Mol. Phys.* **61**, 1487 (1987).
- [21] M. Ross and D. A. Young, *Phys. Lett. A* **118**, 463 (1986).
- [22] R. LeSar, *Phys. Rev. Lett.* **61**, 2121 (1988).
- [23] A. Driessen, E. van der Poll, and I. F. Silvera, *Phys. Rev. B* **33**, 3269 (1986).
- [24] R. J. Hemley, H. K. Mao, L. W. Finger, A. P. Jephcoat, R. M. Hazen, and C. S. Zha, *Phys. Rev. B* **42**, 6458 (1990).
- [25] P. Vinet, J. Ferrante, J. R. Smith, and J. H. Rose, *J. Phys. C* **19**, L467 (1986); *Phys. Rev. B* **35**, 1945 (1987).
- [26] P. Loubeyre, *Physica (Amsterdam)* **139,140B&C**, 224 (1986).
- [27] P. Loubeyre, R. LeToullec, and J. P. Pinceaux, *Phys. Rev. Lett.* **69**, 1216 (1992).